2010

A Novel Far-Field Nanoscopic Velocimetry for Nanofluidics

C. Kuang

Guiren Wang
University of South Carolina - Columbia, wanggu@cec.sc.edu

Publication Info

Published in *Lab on a Chip*, Volume 10, Issue 2, 2010, pages 240-245.

Kuang, C. & Wang, G. (2010). A novel far-field nanoscopic velocimetry for nanofluidics. *Lab on a Chip*, 10(2), 240-245.
http://dx.doi.org/10.1039/B917584A

A novel far-field nanoscopic velocimetry for nanofluidics

Cuifang Kuang and Guiren Wang*

Received 26th August 2009, Accepted 15th October 2009
First published as an Advance Article on the web 17th November 2009
DOI: 10.1039/b917584a

For the first time we have been able to measure the flow velocity profile for nanofluidics with a spatial resolution better than 70 nm. Due to the diffraction resolution barrier, traditional optical methods have so far failed in measuring the velocity profile in a nanocapillary or a closed nanochannel without an opened sidewall. A novel optical point measurement method is presented which applies stimulated emission depletion (STED) microscopy to laser induced fluorescence photobleaching anemometer (LIFPA) techniques to measure flow velocity. Herein we demonstrate this far-field nanoscopic velocimetry method by measuring the velocity profile in a nanocapillary with an inner diameter of 360 nm. The closest measuring point to the wall is about 35 nm. This method opens up a new class of functional measuring techniques for nanofluidics and for nanoscale flows from the wall.

Introduction

With recent progress in microfluidics, nanofabrication and nanotechnology, the field of nanofluidics is now gaining importance in the field of Lab-on-a-Chip.[1,2] Interest in this area is not just motivated by studying increasingly smaller sizes, *i.e.* nanoscale channels, but because there are new areas of fundamental physics, materials science, and chemistry that are important at the nanoscale.[3] For example, biological systems display a plethora of nanomachines, *e.g.*, enzymes and ion channels, which operate in a fluid environment.[4] In fact, transport phenomena can also dramatically change in non-biological nanofluidics compared with that in microscale. In this regard, a recent breakthrough observation is that the flow rate in nanotube membranes can be nearly five orders of magnitude greater than predicted from conventional hydrodynamic theory.[5,6] This important discovery could lead to new understanding of the transport mechanisms in transmembrane protein pores such as aquaporins, methods for selective biochemical sensing, and flow control in nanofluidics. However, the interpretation of high flow rate in nanotube membranes remains an open question.[7] To explain this behavior, slip length with values up to tens of micrometres has been used for modifying the Hagen-Poisseuille equation in a nanotube only several nanometres in diameter.[5,6] An extremely large slip length (micrometre order) inside a very small tube (nanometre order) indicates a nearly flat velocity profile, in contrast to the Hagen–Poiseuille flow model. On the other hand, experiments have also shown an increased flow resistance in nanocapillary filling,[8,9] and the explanation of this increased resistance in nanochannel is not clear either.[9,10]

In order to build functional and practical nanofluidic devices, it is also important to know the velocity profile, which plays an key role for transport phenomenon and separation in nanofluidics, due to, *e.g.* Taylor dispersion.[11] Although there has been considerable research performed in the area of nanofluidics which focused on the study of fluid flow velocity profiles, only theoretical or simulation results exist. The reason for the lack of experimental evidence is simply because no nanovelocimetry currently exists to measure the flow velocity, or even the transient bulk flow velocity in nanofluidic studies, where the transverse dimension is between 1–500 nm. Here, the term nanovelocimetry refers to a device capable of measuring a flow velocity profile with spatial resolution within the range 1–100 nm. Without the capability of measuring the velocity profile in nanochannels, the nanofluidics could be seen as a "black-box", and the relevant research and development of nanofluidic devices will be greatly hampered.

The most successful approaches for employing advanced velocimetry for measurements in microfluidics, are micro-particle image velocimetry (μPIV)[12–16] and molecular tagging velocimetry (MTV)[17–28] respectively. (Note that another high spatial resolution (about 50 nm) method was presented using atomic force microscopy (AFM) by Piorek *et al.*,[29] but due to its intrusive nature and access issue, it could be very difficult to use this technique in a nanochannel that does not have an opened sidewall.) Evanescent wave total internal reflection has been used with nanoPIV (nPIV).[30–34] This method can measure the flow velocity within a distance of 100 nm from the solid wall, and even the velocity distribution near the wall in microchannel.[35] Both μPIV and nPIV use particles whose diameters are of the same order as a nanochannel, and therefore are not suitable in nanofluidics systems since the particles can disturb and block flow and thus are no longer "passive". Furthermore, larger particles could modify the evanescent wave field, the ability of particles to move close to the surface, and particle–fluid interactions could compromise the accuracy of fluid velocity measurement. A quantum dot of 6 nm in diameter has therefore been developed for nPIV.[36] However, so far no report has been published on measuring velocity profiles in nanochannels.

The powerful MTV method uses a molecular tracer and avoids the issues related to nanoparticle tracers. There are several methods employed by MTVs,[25] including caged-fluorescence visualization.[37,38] MTV also includes photobleaching based

Department of Mechanical Engineering & Biomedical Engineering Program, University of South Carolina, Columbia, SC, 29208, USA. E-mail: guirenwang@sc.edu; Fax: +1 803-777-0106; Tel: +1 803-777-8013

methods. Original fluorescence recovery after photobleaching (FRAP), that requires two laser beams at the detection point, has been used to measure extremely low flow velocity in the region of Brownian motion.[39] The method was further developed to measure convection velocity.[26] Since this method has to wait for the recovery of fluorescence, the temporal resolution is relatively low. Photobleached fluorescence visualization[20] and a line writing technique with photobleaching[19] have also been developed to measure flow velocity. The former has relatively low temporal resolution and the latter has difficulty in measuring the velocity profile. A qualitative implementation of photobleaching for flow visualization in a Bénard–Marangoni flow has also been developed.[28] However, no associated quantitative measurement has been developed.

Recently a powerful velocimetry, laser induced fluorescence photobleaching anemometry (LIFPA) has been developed using a molecular tracer with high temporal and spatial resolution to measure the velocity profile in microcapillaries.[40–43] In LIFPA, a molecular tracer of fluorescence dye and the photobleaching effect are applied as a transducer to measure the flow velocity. The velocity is calculated by measuring fluorescence with a calibration relationship between the velocity and fluorescence. The temporal resolution has been achieved to ~5 μs,[44] and it appears that this method has the potential to further improve the temporal resolution.

The most important issue is that all of the aforementioned optical methods (except evanescent wave) have spatial resolutions set by the well known Abbe's diffraction limit on confocal microscopy.[45] Since this normally implies a spatial resolution greater than about 200 nm, these methods cannot directly be used in nanofluidics.

Even though non-intrusive nanovelocimetry is highly desirable, none has been developed that can measure the flow velocity in nanofluidics systems where the transverse dimension in a nanochannel is between 1–500 nm. Neto *et al.*[46] emphasize the strong need for an accurate physical description of fluid flow near an interface with molecular resolution. (However, current techniques do not appear to be capable of yielding such results, and therefore we depend on indirect techniques to infer fluid flow near interfaces, which is very important for nanofluidics.) In order to develop a non-intrusive optical method, relevant key issues must be addressed. (1) The tracer has to be molecular in size. Although a small molecule can be regarded as a particle, its size is generally much smaller than that of a normal nanoparticle. (2) The molecular tracer should be able to serve as a signal transducer to monitor flow velocity if it is based on single point measurement. (3) A novel "focused laser beam" will be required in order to overcome the Abbe's diffraction limit, since the size of the nanochannel is normally the same order or smaller than Abbe's diffraction limit (~200 nm). (4) The optical method should provide far-field nanoscopy, such that several different transverse positions within the nanochannel can be scanned for measuring the velocity profile over a sufficiently long working distance. (5) No "waiting" should be required for either data interrogation or recovery, so that high temporal resolution is achieved.

Several break-through techniques have recently emerged relative to the capability of "focusing" a laser beam to a smaller size than the diffraction limit, thereby increasing spatial resolution for optics-based measurements. Stimulated emission depletion (STED) seems to be the most promising technique for high spatial resolution measurement that is based on far-field nanoscopy and laser induced fluorescence (LIF), and is compatible with LIFPA. Hell[47] pioneered the STED that broke the diffraction barrier and achieved a spatial resolution of about 5.8 nm in the focal plane.[48] STED provides the ability to achieve an extremely finely focused laser beam.

In this letter, we describe an optical point measurement technique, *i.e.* far-field nanoscopic velocimetry, to measure flow velocity profile in a nanocapillary. Here we combine the principle of STED to "focus" the laser beam to overcome the diffraction limit with the principle of LIFPA to measure the velocity.

Measurement mechanism

The measurement principle is based on LIFPA and STED. The current LIFPA method is a single point measurement whose volume is about 2 attolitres. The relation between fluid velocity (V) and fluorescence intensity (I_f) can be expressed as a simplified model[40]

$$I_f = I_{f0} e^{-d/(V\tau)} \quad (1)$$

where constant I_{f0} represents fluorescence intensity at $t = 0$; τ denotes the photobleaching time constant, and the focus laser beam width is d. If I_f is known, the velocity (V) can be calculated using eqn (1). In order to measure the velocity profile in a nanocapillary, a measurement system with nano-scale spatial resolution is required. For this purpose, we developed a continuous wave STED system to overcome the Abbe's diffraction limit, so that a nano-scale resolution can be realized.

STED itself has proven to be a revolutionary technology for far-field, noninvasive nano-scale imaging of fluorescently labeled structures. Fig. 1 illuminates the basic principles of STED. The excitation laser beam (violet light) is steered by a dichroic mirror through an objective lens, and is focused to a spot in the flow field. The smaller the excitation spot, the better the spatial resolution. However, due to diffraction, the detecting zone cannot be made smaller than ~200 nm by the focusing laser beam with a lens, even though the confocal technique is applied. The trick with STED is that one uses a second laser beam (green light), which is doughnut-shaped by a phase plate modulation and concentric over the excitation spot, to quench the fluorescent dye before it can fluoresce, by using the same objective lens. The STED (second laser) is able to preferentially quench the dye at the outer edge of the excitation spot and not that in the center. The result is a smaller effective fluorescence spot. If one defines saturation laser intensity as I_{sat}, at which half of the excited molecules are stimulated to the ground state, the resolution of a STED system (Δx) can be described by:[49]

$$\Delta x = \frac{\lambda}{2n \sin\theta \sqrt{1 + I/I_{sat}}} \quad (2)$$

where λ, n, θ are the beam wavelength, refractive index, and half aperture angle of the lens, respectively. This shows that increasing the intensity (I) of the STED laser, the signal becomes more depleted at the spot's periphery and increasingly more effective towards the middle. In the region of the doughnut hole,

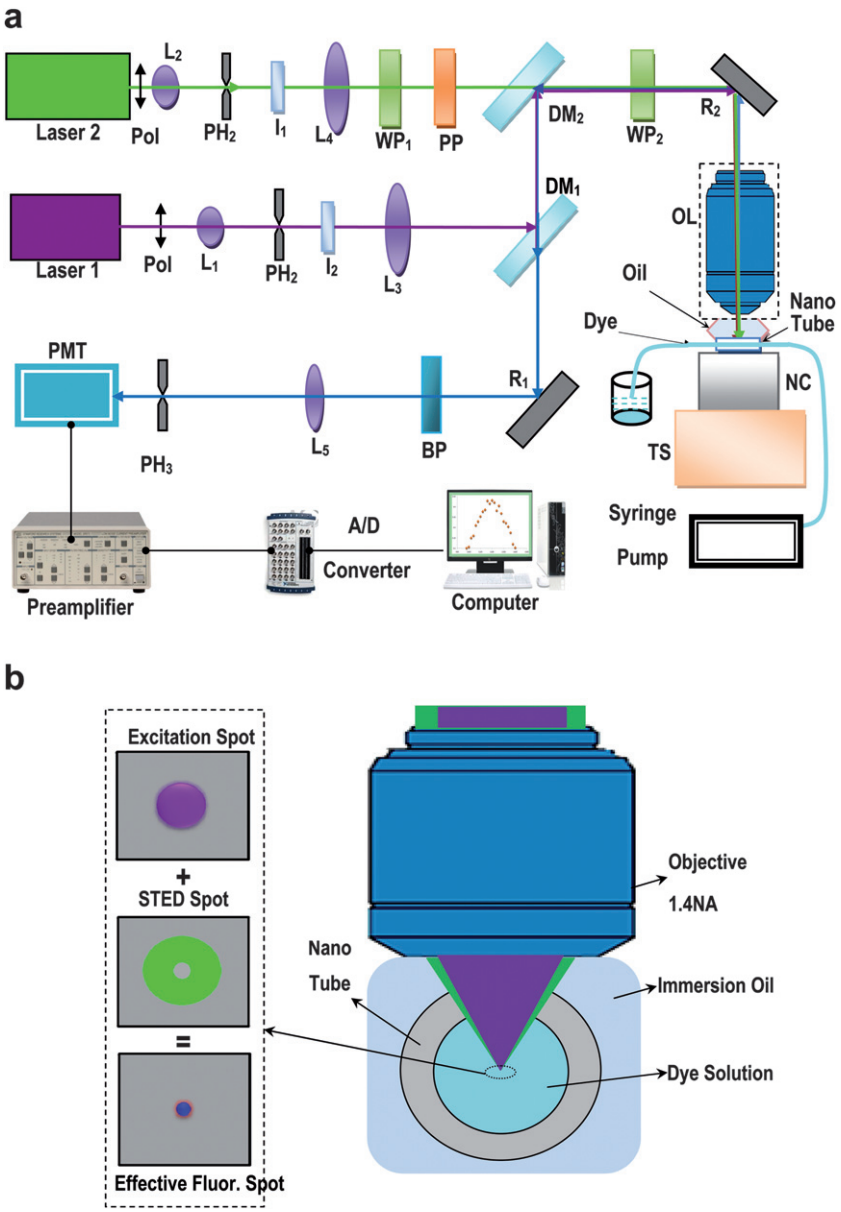

Fig. 1 A schematic of the nanoscopic velocimetry setup. (a) Laser 1: continuous wave at 405 nm; laser 2: continuous wave at 532 nm; L_1, L_2, L_3, L_4 and L_5: optical lenses; PH_1, PH_2 and PH_3: pinholes; I_1 and I_2: Iris; WP_1 and WP_2: wave plate (WP_1: $\lambda/2$, WP_2: $\lambda/4$); Pol: light polarization direction; DM_1 and DM_2: dichroic mirrors; PP: phase plate; PMT: photomultiplier tube; R_1 and R_2: reflector mirrors; BP: bandpass filter; OL: objective lens (PlanApo 100X, NA = 1.4 oil immersion); dye: Coumarin 102; NC: nano cube piezo scanner (3-axis); TS: translation stage (3-axis). (b) A detailed sketch of the measurement setup in the vicinity of the nanocapillary.

however, the fluorescence is ideally not affected at all. Therefore, by increasing the intensity of the doughnut-shaped second STED beam, the fluorescence spot (measurement point) can be progressively narrowed.[47–51]

Measurement system

We will now describe the system and equipment needed for this approach. The schematic of the experimental setup is shown in Fig. 1a. The excitation beam (laser 1) is generated by a continuous wave (CW) violet laser diode with a wavelength of 405 nm. The linear-polarized beam is aligned through a lens–pinhole–lens system which includes lens (L_1), pinhole (PH_1) and lens (L_3) to expand the beam diameter. A dichroic mirror (DM_1) reflects the beam and the latter is reflected by a second dichroic mirror (DM_2). On the other hand, the STED beam (laser 2) is generated by a CW green laser diode with a wavelength of 532 nm. The linear-polarized STED beam is cleaned and expanded by another lens-pinhole-lens system which includes lens (L_2), pinhole (PH_2) and lens (L_4). The STED beam is then transmitted by a $\lambda/2$ wave plate which can make the polarized direction same to that of the excitation beam. Downstream of the phase plate (PP) and DM_2, the two laser beams mentioned combine and pass through a $\lambda/4$ wave plate. Orientation of the fast axis of the $\lambda/4$ wave plate is set to 45° with reference to the polarized direction. The linear polarization state of the beam is changed to circular by this wave

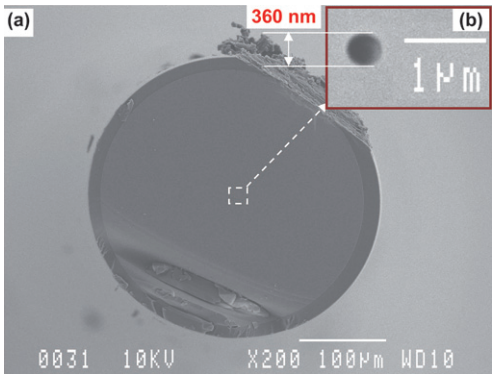

Fig. 2 Image for cross-section of nanocapillary by a SEM microscope. (a) At 200× magnification; (b) this magnified view of the marked area demonstrates the nano-scale capillary at 10 000× magnification. (Courtesy of Polymicro Technology.)

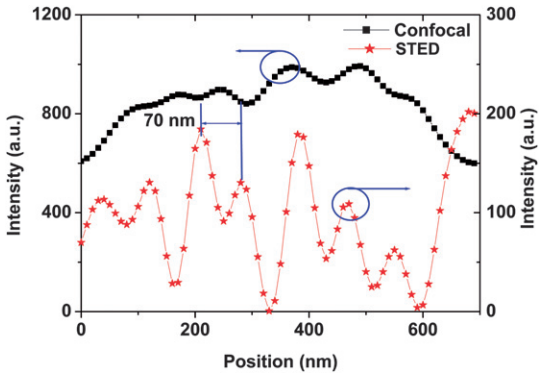

Fig. 3 Comparison of spatial resolution between the CW STED system and confocal microscope. The fluorescence intensity profile of nanoparticles is measured to determine the smallest distance between two peaks that can be discriminated when the "focused" laser beam scans through various positions along a line.

plate. The circular polarization beams are reflected by a reflector (R_2) and focused by an objective lens (OL, 100X, PlanApo, NA 1.4 oil immersions). Fig. 1b is a detailed sketch of the measurement setup in the vicinity of the nanocapillary. It illustrates patterns of the excitation and STED in the objective focal plane.

In order to facilitate the following theoretical prediction that is used to compare with the experimental results, the inner diameter (ID) of the nanocapillary was measured by a scanning electron microscope (SEM). The cross-section image of the nanocapillary is shown with 200× magnification in Fig. 2(a). The inset image (b) is a magnified view of the marked area, and demonstrates the nanoscale tube at 10 000× magnification. From the inset image Fig. 2(b), it can be seen that the ID of this nanocapillary is about 360 nm.

A nanocapillary with inner diameter of 360 nm is fixed on a nanocube (NC) piezo-scanning stage that can be translated in all three spatial directions with a positioning resolution of 1 nm for fine-tune. Another 3-axis manual translation stage (TS) is used for rough adjustment. A fluorescent dye is used to generate fluorescence. The fluorescence emitted by the dye is collected by the same objective lens and passes the two dichroic mirrors (DM_1 and DM_2). Then it is reflected (R_1) and focused onto a photomultiplier tube (PMT) by a lens (L_5). The fluorescence signal is detected confocally through a confocal pinhole. The pinhole and an optical bandpass filter for the fluorescence signal are placed before the detector. The reason for using a pinhole is to reject stray and ambient light to reduce noise. The signal from the detector is amplified by a current preamplifier, and then acquired by an A/D converter and saved to a computer.

Experimental results and discussion

We will now describe the experiments used to validate this new far-field nanoscopic velocimetry. To determine the effective spatial resolution, we scanned a glass cover slide coated with fluorescence nanoparticles (~100 nm, Spherotech Inc.) using both the STED and confocal techniques. These particles are distributed randomly on the slide. The resolution is defined as the smallest distance between two distinguished peaks. Hence, it is very difficult to find the smallest distance between two particles, which the STED system can distinguish. From Fig. 3, it can be seen that the STED system has achieved a spatial resolution better than 70 nm in the focal plane, while the confocal technique cannot discriminate the two peaks from the particles.

To validate the feasibility and accuracy of this far-field nanoscopic velocimetry system for measuring velocity profile, a series of experiments were performed. All of the parts of the experimental system (see Fig. 1) were fixed on an optical table. A nanocapillary of 360 nm ID was fixed on the NC piezo-scanning stage. First this velocity measurement technique requires calibration between fluid velocity and fluorescence intensity. The calibration process was the same as described in our previous work.[43] Fig. 4 shows the experimentally measured relationship between flow velocity and observed fluorescence intensity. Black squares represent the measured result for the calibration between velocity and fluorescence intensity. Three runs were made for each measuring point to generate these average points. The standard deviation error bars are given in Fig. 4 as well. Based on the experimental data in Fig. 4, a polynomial correlation of the calibration points for the setup was obtained.

After calibration, nanocapillary fluid measurements were performed by moving the NC piezo stage in the radial direction through the axis of the nanocapillary. The nanocapillary width is traversed in 18 steps; each step is only 20 nm. The time it takes to

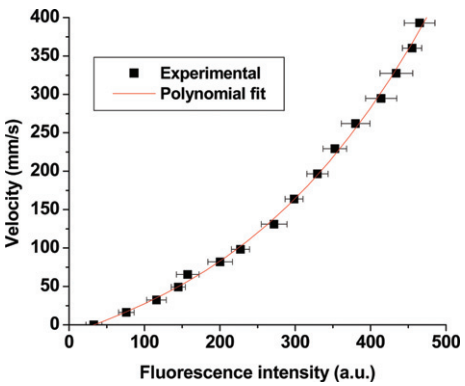

Fig. 4 The calibrated relationship between fluorescence intensity and flow velocity measured in the centerline of the nanocapillary.

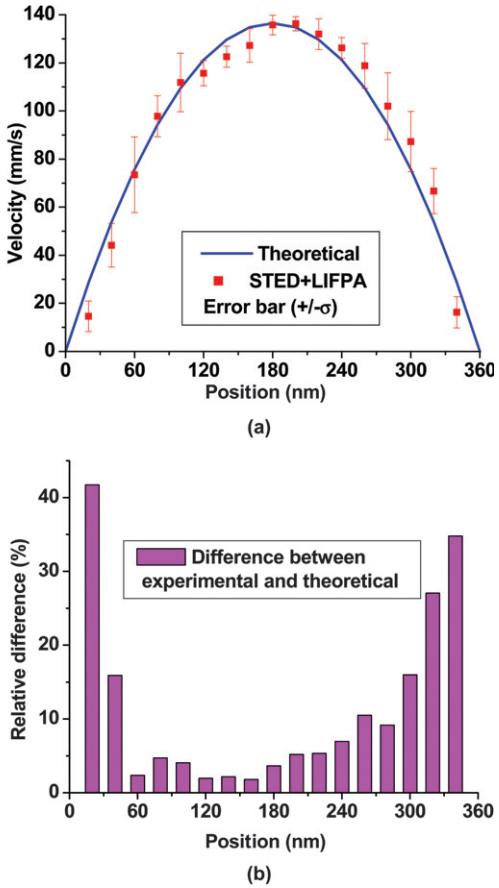

Fig. 5 Velocity profile and relative difference. (a) Velocity profile in a nanocapillary of 360 nm ID; (b) relative difference between the experimental results and theoretical prediction (parabolic).

perform a point measurement and one scan across the diameter is 0.2 s and about 4 s, respectively. The positional results are averaged using five runs. Based on the relationship between the intensity and velocity, the velocity profile of the nanocapillary is attained as shown in Fig. 5(a), where rectangular dots represent the average velocity of the measurement point. The standard deviation error bars are also shown in Fig. 5(a). In order to validate the method, theoretical prediction based on the Hagen–Poiseuille equation is used to compare with the experimental results. For a constant pressure gradient in the axial direction of the nanocapillary with no-slip boundary condition at the wall, this theoretical velocity profile can be expressed as:[52]

$$V(r) = \frac{2Q}{\pi R^2}\left[1 - \left(\frac{r}{R}\right)^2\right] \quad (3)$$

where V is the fluid velocity in the axial direction, R is the radius of the nanocapillary, r represents the distant between the measurement point and the axis of the nanocapillary and Q denotes the volumetric flow rate (which is set to 0.0004 μl h^{-1} here). The difference between the experimental data and theoretical prediction is given in Fig. 5(b). What is important is that, for the first time, the velocity profile in a nanocapillary can now be directly measured. The measurement result is an approximation to the parabolic Poiseuille flow profile, which is basically similar to the theoretical prediction. The measured velocity profile in Fig. 5(a) could indicate that at least the classical Hagen–Poiseuille equation could still be valid when the capillary ID is 360 nm. The velocity can clearly be differentiated within just a 20 nm step, even near the axial region of the nanocapillary. The closest measuring point to the wall is estimated to be about 35 nm. Clearly, the technique can be applied not only in nanofluidics, but also in near-wall interfacial flows.

Note that the difference increases as the measuring points are approaching the wall of the nanocapillary. This phenomenon might be explained as follows. (1) The total internal reflection phenomenon is partially generated in the nanocapillary due to the mismatch of the refraction index between the fluid and the wall. Evanescent waves have an intensity that decays exponentially along the distance normal to the interface.[35] This error could be decreased if the nanochannel were rectangular, and if the refraction index of the capillary wall and the fluid were the same. (2) The calibration could also be an error source, since the calibration is conducted only on the axis. Such an error could be reduced if time-of-flight[17,18] is also used for the calibration. (3) In addition, in a nanoscale capillary, the real velocity profile might be different from the prediction of classical theory.[8–10]

Conclusions

STED itself has proven to be a revolutionary technology for far-field, noninvasive nanoscale imaging of fluorescently labeled structures.[47–49,51] Concurrently the LIFPA is a promising technique for velocity measurement.[43,53] Applying STED to LIFPA could establish a new method for nanoscopic velocity measurement that can 'side-step' the classical optical diffraction limit.

In conclusion, we presented and demonstrated a far-field nanoscopic technique to successfully measure flow velocity in nanofluidics. This nanovelocimetry, applying STED to LIFPA, enables direct experimental measurement of flow velocity profile in nanofluidics beyond the diffraction limit. The closest measuring point from the wall is estimated to be about 35 nm. The corresponding spatial resolution is better than 70 nm. This method opens up a new opportunity for research in nanofluidics and interfacial flows.

Acknowledgements

This work has been financially supported by the NSF RII funding (EPS-0447660). The authors thank Dr Jeff Morehouse for editing this manuscript. The discussion with colleague Wei Zhao is also appreciated.

References

1 A. Piruska, S. Branagan, D. M. Cropek, J. V. Sweedler and P. W. Bohn, *Lab Chip*, 2008, **8**, 1625–1631.
2 Y.-J. Oh, D. Bottenus, C. F. Ivory and S. M. Han, *Lab Chip*, 2009, **9**, 1609–1617.
3 R. Mukhopadhyay, *Anal. Chem.*, 2006, **78**, 7379–7382.
4 M. Rauscher and S. Dietrich, *Annu. Rev. Mater. Res.*, 2008, **38**, 143–172.
5 M. Majumder, N. Chopra, R. Andrews and B. J. Hinds, *Nature*, 2005, **438**, 44.
6 J. K. Holt, H. G. Park, Y. Wang, M. Stadermann, A. B. Artyukhin, C. P. Grigoropoulos, A. Noy and O. Bakajin, *Science*, 2006, **312**, 1034–1037.
7 D. Mattia and Y. Gogotsi, *Microfluid. Nanofluid.*, 2008, **5**, 289–305.

8 E. Tamaki, A. Hibara, H.-B. Kim, M. Tokeshi and T. Kitamori, *J. Chromatogr., A*, 2006, **1137**, 256–262.
9 N. R. Tas, J. Haneveld, H. V. Jansen, M. Elwenspoek and A. van den Berg, *Appl. Phys. Lett.*, 2004, **85**, 3274–3276.
10 J. Ralston, M. Popescu and R. Sedev, *Annu. Rev. Mater. Res.*, 2008, **38**, 23–43.
11 R. B. Schoch, J. Han and P. Renaud, *Rev. Mod. Phys.*, 2008, **80**, 839–845.
12 J. G. Santiago, S. T. Wereley, C. D. Meinhart, D. J. Beebe and R. J. Adrian, *Exp. Fluids*, 1998, **25**, 316–319.
13 S. M. Hagsater, A. Lenshof, P. Skafte-Pedersen, J. P. Kutter, T. Laurell and H. Bruus, *Lab Chip*, 2008, **8**, 1178–1184.
14 Y. Liu, M. G. Olsen and R. O. Fox, *Lab Chip*, 2009, **9**, 1110–1118.
15 H.-W. Lu, F. Bottausci, J. D. Fowler, A. L. Bertozzi, C. Meinhart and C.-J. C. Kim, *Lab Chip*, 2008, **8**, 456–461.
16 H. Kinoshita, S. Kaneda, T. Fujii and M. Oshima, *Lab Chip*, 2007, **7**, 338–346.
17 J. L. Pittman, C. S. Henry and S. D. Gilman, *Anal. Chem.*, 2003, **75**, 361–370.
18 J. L. Pittman, S. D. Gilman and K. F. Schrum, *Analyst*, 2001, **126**, 1240–1247.
19 K. F. Schrum, J. M. Lancaster, S. E. Johnston and S. D. Gilman, *Anal. Chem.*, 2000, **72**, 4317–4321.
20 B. Mosier, J. Molho and J. Santiago, *Exp. Fluids*, 2002, **33**, 545–554.
21 A. W. Moore and J. W. Jorgenson, *Anal. Chem.*, 1993, **65**, 3550–3560.
22 B. Flamion, P. M. Bungay, C. C. Gibson and K. R. Spring, *Biophys. J.*, 1991, **60**, 1229–1242.
23 H. Hu and M. M. Koochesfahani, *Meas. Sci. Technol.*, 2006, **17**, 1269.
24 R. E. Falco and D. G. Nocera, ed. M. C. Rocco, London, Butterworth-Heinemann, 1993.
25 M. M. Koochesfahani and D. G. Nocera, *Molecular Tagging Velocimetry. Handbook of Experimental Fluid Dynamics. Chapter 5.4*, Springer-Verlag, Heidelberg, 2007.
26 P. H. Paul, M. G. Garguilo and D. J. Rakestraw, *Anal. Chem.*, 1998, **70**, 2459–2467.
27 A. E. Herr, J. I. Molho, J. G. Santiago, M. G. Mungal, T. W. Kenny and M. G. Garguilo, *Anal. Chem.*, 2000, **72**, 1053–1057.
28 J. Rička, *Exp. Fluids*, 1987, **5**, 381–384.
29 B. Piorek, A. Mechler, R. Lal, P. Freudenthal, C. Meinhart and S. Banerjee, *Appl. Phys. Lett.*, 2006, **89**, 153123–153123.
30 H. Gai, Y. Li, Z. Silber-Li, Y. Ma and B. Lin, *Lab Chip*, 2005, **5**, 443–449.
31 C. Zettner and M. Yoda, *Exp. Fluids*, 2003, **34**, 115–121.
32 K. D. Kihm, A. Banerjee, C. K. Choi and T. Takagi, *Exp. Fluids*, 2004, **37**, 811–824.
33 S. Jin, P. Huang, J. Park, J. Y. Yoo and K. S. Breuer, *Exp. Fluids*, 2004, **37**, 825–833.
34 H. Li, R. Sadr and M. Yoda, *Exp. Fluids*, 2006, **41**, 185–194.
35 D. Duong-Hong, J.-S. Wang, G. Liu, Y. Chen, J. Han and N. Hadjiconstantinou, *Microfluid. Nanofluid.*, 2008, **4**, 219–225.
36 S. Pouya, M. Koochesfahani, A. Greytak, M. Bawendi and D. Nocera, *Exp. Fluids*, 2008, **44**, 1035–1038.
37 D. Ross, T. J. Johnson and L. E. Locascio, *Anal. Chem.*, 2001, **73**, 2509–2515.
38 J. I. Molho, A. E. Herr, B. P. Mosier, J. G. Santiago, T. W. Kenny, R. A. Brennen, G. B. Gordon and B. Mohammadi, *Anal. Chem.*, 2001, **73**, 1350–1360.
39 J. White and E. Stelzer, *Trends Cell Biol.*, 1999, **9**, 61–65.
40 G. R. Wang, *Lab Chip*, 2005, **5**, 450–456.
41 G. R. Wang and H. Jiang, US patent, 7283215, 2007.
42 G. R. Wang, I. Sas, H. Jiang, W. P. Janzen and C. N. Hodge, *Electrophoresis*, 2008, **29**, 1253–1263.
43 C. Kuang, W. Zhao, F. Yang and G. Wang, *Microfluid. Nanofluid.*, 2009, **7**, 509–517.
44 C. Kuang and G. R. Wang, Ultrafast Measurement of Transient Electrokinetic Flow in Microfluidics, 2009, submitted.
45 Y. Kuznetsova, A. Neumann and S. R. Brueck, *Opt. Express*, 2007, **15**, 6651–6663.
46 C. Neto, D. R. Evans, E. Bonaccurso, H.-J. u. Butt and V. S. J. Craig, *Rep. Prog. Phys.*, 2005, **68**, 2859–2897.
47 S. W. Hell, *Nat. Biotechnol.*, 2003, **21**, 1347–1355.
48 E. Rittweger, K. Y. Han, S. E. Irvine, C. Eggeling and S. W. Hell, *Nat. Photonics*, 2009, **3**, 144–147.
49 G. Donnert, J. Keller, R. Medda, M. A. Andrei, S. O. Rizzoli, R. Lührmann, R. Jahn, C. Eggeling and S. W. Hell, *Proc. Natl. Acad. Sci. U. S. A.*, 2006, **103**, 11440–11445.
50 K. Y. Han, K. I. Willig, E. Rittweger, F. Jelezko, C. Eggeling and S. W. Hell, *Nano Lett.*, 2009, **9**(9), 3323–3329.
51 E. Rittweger, B. R. Rankin, V. Westphal and S. W. Hell, *Chem. Phys. Lett.*, 2007, **442**, 483–487.
52 F. M. White, *Viscous Fluid Flow*, McGraw-Hill, New York, 1991.
53 C. Kuang, F. Yang, W. Zhao and G. Wang, *Anal. Chem.*, 2009, **81**, 6590–6595.